DOI: 10.13009/EUCASS2019-244

Optimization of the base bleed to control trailing edge flows in a wide range of Mach numbers

Alejandro Martinez-Cava[1†], *Eusebio Valero*[1], *Jorge Saavedra*[2], *Francisco Lozano*[2] *and Guillermo Paniagua*[2]
[1]*School of Aeronautical and Space Engineering, Universidad Politécnica de Madrid.*
Plaza Cardenal Cisneros 3, E-28040, Madrid, Spain
[2]*Purdue University, West Lafayette, IN, United States*
[†]Corresponding author: alejandro.martinezcava@upm.es

Abstract

Turbine blade cooling can be exploited to modulate the flow between turbine stages. The current manuscript explores the potential use of base-bleed control, with the aim of reducing the pressure losses in transonic and supersonic turbines, while enhancing the thermal protection along the trailing edge surface. Older research constrained to low Mach numbers is now explored in a significantly broader range of Mach numbers. Pulsating base bleed techniques are compared against constant blowing and non-blowing configurations, showing a great potential on the modulation of the flow structures and coolant flow mixing.

1. Introduction

In the pursue of higher performance, aircraft engine architectures tend to compact and lighter designs, where the force stresses and internal temperatures push the materials to their limits. In particular, high outlet Mach number turbine engines experiment high fluctuating aerodynamic loads due to the complex flow systems that develop between turbine stages. The trailing edge shock waves from one row, impact on the one downstream, and may impact the performance of neighbouring airfoils. Moreover, the relative movement of one row induces oscillating loads, caused by the moving blockage, and unsteady movement of the shocks, severely impacting the fatigue life.[1]

A schematic description of the flow topology is shown in Figure 1. As the boundary layers from upper and lower side of the turbine blade reach the trailing edge, they separate in two alternate shear layers that join again downstream of the blade in a confluence point. They form a low pressure and low momentum area between the blade trailing edge and the confluence point, known as the base region. The properties of this area strongly affect the flow topology downstream of the blade. The alternate separation of the shear layers generate one or more pairs of vortices, depending on the Reynolds number, that travel downstream forming a vortex street. In transonic or supersonic configurations this is accompanied by the presence of expansion and compression waves that adapt the flow between turbine stages. A Prandtl expansion fan develops at the trailing edge, accelerating the flow that is later recompressed in a strong trailing edge shock with its foot at the point of confluence of the two shear layers. Additionally, a pair of weak shock waves develop at the base region together with the shear layers, namely the lip shock waves.

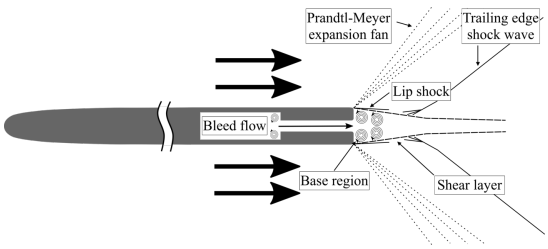

Figure 1: Schematic representation of the high speed complex flow topology around a trailing edge.

The extreme temperatures reached inside turbines operating at high Mach number require continuous blade cooling to avoid damage of the turbine elements. The trailing edge of the blades are normally very thin, such that no cooling passages can be fitted inside, and they are refrigerated by constant blowing of coolant flow through holes or slots. This flow ejection can be exploited to control the flow topology around the turbine blade trailing edge and to control the properties of the base region.[2] Several studies contemplate the use of base bleed coolant ejection on the mitigation of wake vortex shedding phenomenon or the shock wave intensities.[3–6] An additional step in this direction was the modulation of the base bleed flow, using a pulsating coolant jet instead of a constant mass flow. Flow control using pulsating base bleed has been already studied in low supersonic regime.[7–9] Some numerical analyses suggested that pulsating base bleed was not as beneficial as constant blowing[8] in terms of reducing the shock wave intensities

Copyright © 2019 by Martinez-Cava et al. Published by the EUCASS association with permission.

DOI: 10.13009/EUCASS2019-244

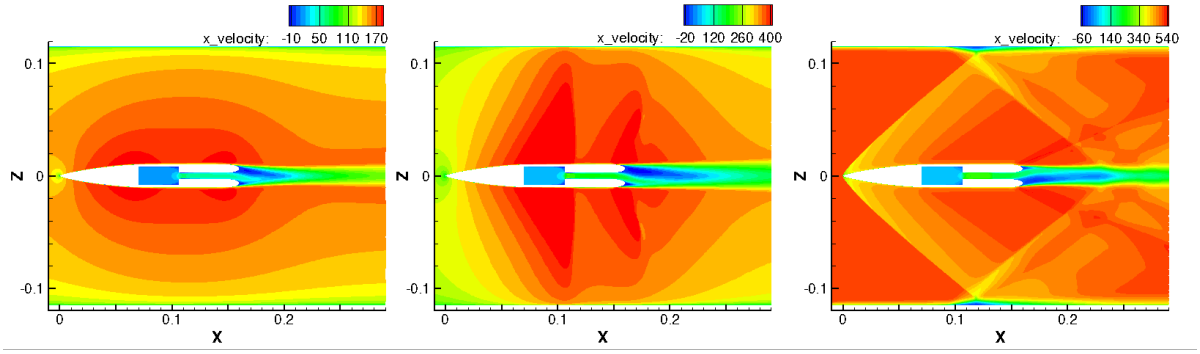

Figure 2: Streamwise velocity contours for constant base bleeding in the three sonic regimes. A *Coanda* effect at the end of the injection channel can be observed in the three configurations. Image modified from Martinez-Cava et al.[11]

and increasing the base pressure. However, experimental data indicates that pulsating base bleed can enhance blade cooling and reduce the losses generated by the impingement of the shock wave on the suction side of the blades in the next turbine stage.[9,10]

This research is a continuation of the work of Martinez-Cava et al.,[11] where the apparition of a symmetry breaking effect on a trailing edge base bleed due to a global instability was investigated. When flow is ejected at the trailing edge, a global instability may become unstable for certain blowing intensities, breaking the symmetry of the jet. This was first observed by Saracoglu et al.[6] in supersonic turbine blade configurations, and confirmed by Martinez-Cava et al.[12] by a combination of RANS solutions and stability analysis. The topology at the base region can make flow perturbations to grow in time and eventually generate an alternate flow configuration. The flow symmetrically ejected at the trailing edge modifies its direction due to a *Coanda* effect, generated either by the pressure gradient present at the wall or by the pressure difference between the upper and lower parts of the base region (Fig. 2). In subsonic and transonic configurations, this phenomenon was also linked with the damping of the vortex shedding downstream of the turbine blade. It was observed that the *Coanda* effect was present at only certain blowing intensities, linked with a vortex shedding damping, but disappearing when the jet intensity increased, forcing the flow to recover its symmetry. Depending on the shape of the trailing edge, the vortex shedding may reappear or the downstream flow may remain steady. However, these studies were restricted to constant base bleed, and the possibilities and potential of pulsating base bleed were not considered.

In this paper three sonic regimes are examined, subsonic, transonic and supersonic, evaluating the influence of pulsating coolant flow base bleeding. The trailing edge mass flow has been selected from the literature,[11] to be such that a *Coanda* effect appears at the trailing edge due to the present global instability. Results are also evaluated for a configuration with a higher base bleed intensity, where the *Coanda* effect is no longer present, but the flow remains without shedding. A range of flow solutions with varying base bleed frequency between 100Hz and 1KHz are compared against constant blowing conditions. The wake structure, mixing of the coolant flow, pressure gradients, and intensity and position of the trailing edge shock waves are measured for all cases. We anticipate that despite the reduced effect that pulsating base bleed has on the base region compared with constant blowing, the effects downstream the model are not negligible at all. For the three sonic scenarios analyzed, notable changes in the shock waves angle, pressure losses and measured forces are found. This analysis is the second numerical contribution in the context of a larger numerical and experimental campaign in close collaboration with the Purdue Experimental Turbine Aerothermal Laboratory (PETAL), where state-of-the-art experimental facilities[13] are used to verify and correlate these results.

The rest of the paper is organized as follows. Section 2 introduces the numerical approach for the calculation of the flow solutions and its analysis, with the results being presented in Section 3. Section 4 closes the paper with the main conclusions of this research.

2. Numerical procedure

All the flow calculations are computed with the Finite Volume DLR-TAU Code[14] (TAU). The solver is a state-of-the-art commercial software, developed for the prediction of viscous and inviscid flows on complex geometries from the low subsonic to the hypersonic flow regime. The flow solver is a three-dimensional, parallel, and multigrid code, that employs a finite volume scheme to solve the compressible flow Reynolds-Averaged Navier-Stokes (RANS) equations. The inviscid terms are computed either with a central or with a second-order upwind scheme, whereas the viscous terms are computed with a second-order central scheme. For time-accurate solutions, TAU uses a dual time-stepping

DOI: 10.13009/EUCASS2019-244

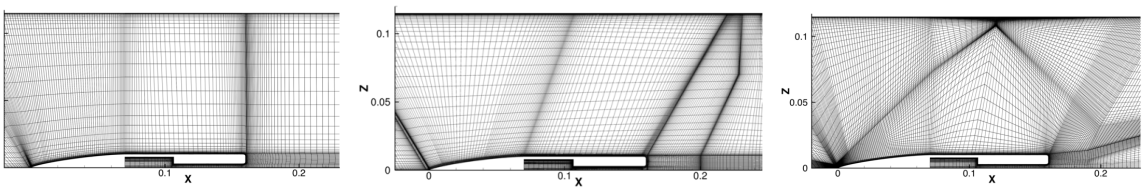

Figure 3: Spatial discretization used on the numerical analysis. Meshes correspond to subsonic (left), transonic (center) and supersonic (right) conditions. Only a quarter of the total nodes is shown for clarity.

scheme. To model the turbulent fluxes, the Menter's Shear Stress Transport version of the k-ω[15] turbulence model is used.

The geometry of the body of analysis is the same that the one used in Martinez-Cava et al.,[11] which design took into account the further validation of the numerical data through extensive experimental testing. The body consisted on a zero-camber airfoil of 160 mm chord (c) inside a linear test section, with a fitness ratio of $c/d = 8$. A Haack Series nose shape was chosen to adapt the flow without any detachments or very strong gradients. The geometry of the two-dimensional model and the wind tunnel walls are included on the computational domain, with far inflow and outflow limits to avoid non-physical boundary interactions. Three different sonic regimes are considered, with an optimised mesh topology for each configuration (Fig. 3). The structured numerical meshes were locally refined to properly capture the wake structure, and the expansion and compression waves. Subsonic conditions at the inlet are generated with a Mach number of 0.4; a flow with a Mach number of 1.1 at the trailing edge of the model is chosen for the transonic regime; and an inflow speed of Mach 2 is used for supersonic flow analysis. The outlet boundary acts either as a direct extrapolation in case of supersonic flow velocity, or imposing ambient pressure if the flow has subsonic conditions.

Base bleed actuation is modelled through the injection of cooler air at an internal plenum chamber of the trailing edge, such that subsonic conditions are kept in the injection, and then redirected to the base region by means of a thinner slot that connects with the outer surface through a curved surface. The shape of the slot end is chosen to be rounded (joining the upper and lower surface through a superellipse) instead of having a straight end, so a full *Coanda* effect could be generated for certain jet intensities.

The evaluation of the Unsteady RANS (URANS) flow solutions is done via the analysis of wake point profiling locations, together with the evaluation of flow variables in several sections of the domain. Each time snapshot of the flow solution is post-processed to extract the information required for the analysis. The interpolation of the unstructured data to the intersection lines is done using in-house *Python* tools.

2.1 Actuation details

Frequency modulating of the cooling flow jet is performed through the *Actuation* boundary condition available in TAU. The mass flow injection is modulated in frequency with a smoothed step function, oscillating from constant blowing to zero-mass flow during one cycle. The variation of the velocity with the actuation cycle is illustrated in Figure 4-(a). The actuation period is defined as $T_f = T_h + T_l$, T_h being the high flow rate time and T_z the zero flow rate. The duty cycle, defined as T_h/T_f, is set to 0.5 for all the cases studied herein. We use a constant actuation model ($U_{jet} = U_{jet-MAX}$ for all T_h) with a signal smoothing to avoid a sharp jump in the injected mass flow (Fig. 4-(a)). The desired mass flow for the injection was obtained from early calculations, where the flow conditions were defined from the relation between the injected flow and the free stream total pressure. This served to generate an injection parameter, $C_b = p_{0purge}/p_{0\infty}$, to define the different states of the base bleed.

There is a strong relation between the mass flow ejected at the trailing edge and the base pressure, with demonstrated gains for low mass flow injections that are quickly damped when the mass flow increases.[6] This study contemplates the application of two different coolant jet intensities, as notable differences are expected. A first configuration, with lower intensity, correlates with the minimum base pressure values obtained for constant trailing edge blowing,[6,11] whereas a second one is chosen to have a higher mass flow rate, and therefore a higher associated base pressure. Both configurations are tested for constant blowing, and for a range of pulsating base bleed frequencies from 100 to 1000Hz. As a rounded trailing edge is considered, a *Coanda* effect will appear at certain coolant jet intensities due to the presence of a global instability.[11] The influence of the *Coanda* effect in the flow topology is also investigated in this paper.

DOI: 10.13009/EUCASS2019-244

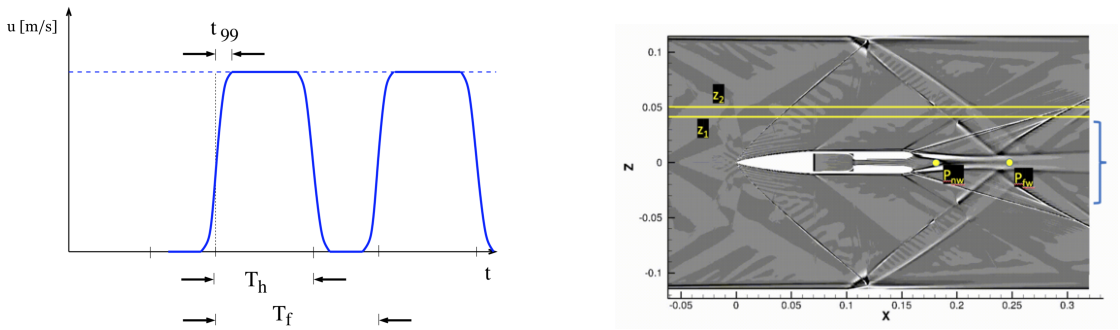

Figure 4: (a):Illustration of the actuating boundary condition for periodic base bleed. (b):Regions for shock intensity and angle evaluation (splines z_1 and z_2), and profiling wake points (P_{nw} and P_{fw}).

2.2 Wake flow and shock wave evaluation

Pulsating base bleed generates notable changes in the base region, but our interest is on evaluating the magnitude of the flow variations downstream the turbine blade. To do so, we monitor frequency variations which are characterized by pressure fluctuations in two points located in the symmetry plane. The two profiling points evaluate near-wake flow properties (P_{nw}, separated a distance of d from the trailing edge) and far-wake flow properties (P_{fw}, located $5d$ downstream from the trailing edge), as illustrated in Figure 4-(b). In addition, the flow losses are measured by the evaluation of a linear cross section located a distance equal to the model chord downstream the model. Data is measured in the linear section $-2d < z < 2d$, focusing in temperature and total pressure losses variations along time.

Following a similar procedure, two linear sections located at different heights (z_1 and z_2) from the model are extracted from the flow solution at each time snapshot. The position and angle of the shock waves are extracted from the maximum values of the density gradient magnitude, which is also used to calculate the variation of the intensity of the shock wave as a percentage variation of the non-base bleed configuration:[8]

$$\Delta \boldsymbol{I}[\%] = \frac{\overline{\max(\|\nabla\rho\|)}_{\mathbf{z1-z2}} - \overline{\max(\|\nabla\rho\|)}_{\mathbf{z1-z2,NB}}}{\overline{\max(\|\nabla\rho\|)}_{\mathbf{z1-z2,NB}}} \cdot 100 \tag{1}$$

Finally, pressure and viscous forces are measured over time to evaluate the influence of the changes generated by the pulsating base bleed actuation.

3. Results and discussion

Pulsating base bleed seems to have a big effect compared to constant trailing edge blowing and no-blowing configurations. However, the three different sonic regimes require different evaluation procedures, due to the various encountered flow topologies. For the sake of clarity, this section is therefore divided in three independent parts.

3.1 Subsonic conditions

The trailing edge flow in subsonic regime is mainly dominated by pressure fluctuations, generated by the trailing edge vortex shedding. With a characteristic Strouhal number of $St = 0.27$, the boundary layers of upper and lower side separate in an alternate manner forming a clear Von-Karman vortex street. A constant trailing edge blowing eliminates the shedding. However, the intermittent ejection of coolant flow does not keep the shedding from its onset, but modulates its intensity and frequency. The effects of the pulsating base bleed on a purge cycle can be observed in Figure 5, where vorticity contours are used to illustrate the detachment of the eddies from the trailing edge. With a continuous shedding, the injection at the base region generates an elongation of the recirculation area, spacing the distance between the vortices ($t = 1/6T$ to $t = 3/6T$). When the ejection finishes, the distance between the vortices decreases, but at the same time two additional small vortices are detached from the injection duct ($t = 4/6T$).

Downstream effects measured on the wake do not show significant variations in the total pressure drop or temperature changes for any of the analyzed frequencies or blowing intensities. However, the drag coefficient shows a strong relation with the frequency of injection. Figure 6 compares the drag coefficient measured for a non-blowing configuration (NB) with the forces measured for the two base bleed intensities. While there is a considerable drag reduction due to the injection of coolant flow at the base region, with even higher reductions achieved with pulsating

DOI: 10.13009/EUCASS2019-244

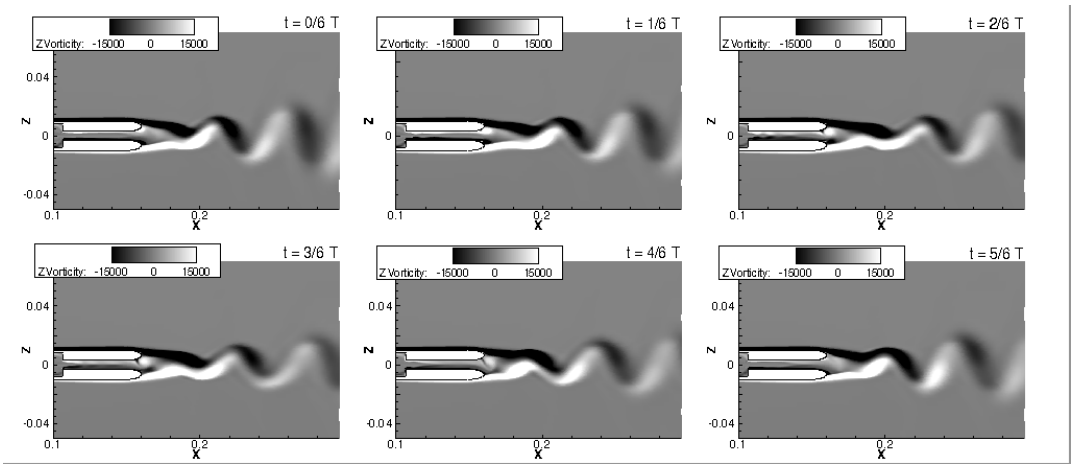

Figure 5: Vorticity contours time snapshots taken along a period of actuation. Subsonic flow, $C_b = 0.9$, $F = 400Hz$.

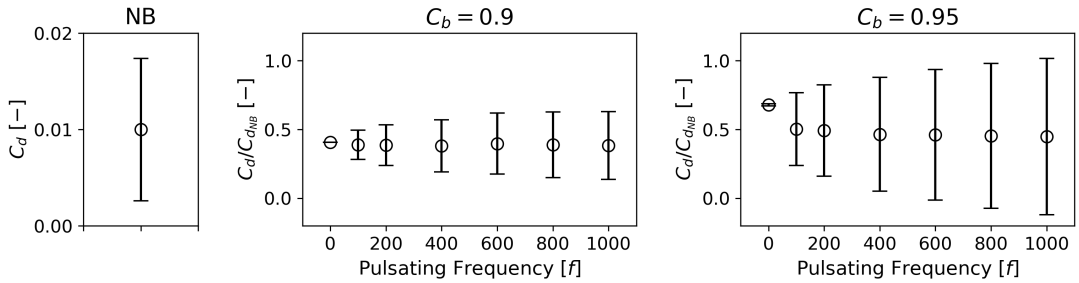

Figure 6: Relation of the drag coefficient with the frequency of actuation. Circular symbols (◯) are used for blowing intensities of $C_b = 0.9$, and square symbols (□) for $C_b = 0.95$. Average values with error bars (RMS) are shown for all the cases.

injection, this reduction does not seem to improve when the frequency is increased. On the other hand, drag oscillations do increase with the frequency, changing from the steady state obtained from constant blowing to oscillations of more than 50% of the reference drag value for the highest frequency base bleed cases. Higher mass flow rates are also related with higher oscillations in the drag coefficient. These changes are due to variations in the pressure drag, as the viscous drag remains almost constant during the injection cycles.

The frequency analysis of the wake profiling points remark the downstream influence of the pulsating blowing, as the dominant frequency oscillating corresponds with the frequency of coolant ejection for all the studied cases (Figures 7 and 8). Interestingly, the frequency of oscillation of the non-actuated wake (St=0.26,[11] measured by lift forces on the model) is not recovered as the one with highest amplitude. An amplitude peak at 600Hz corresponds with the internal acoustic resonance of the cavity injection when no base bleed is applied, with its harmonics appearing in the frequency spectrum and blinding the main wake frequency. This was an unexpected find and will be taken into account in further analyses.

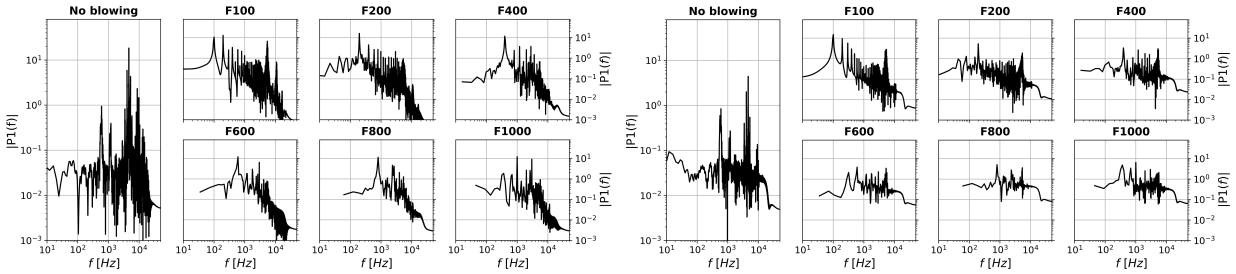

Figure 7: Frequency spectrum of the near-wake profiling point (left) and far-wake profiling point (right). Subsonic regime, $C_b = 0.9$. Constant flowing frequency sprectrum is ommited as the flow is steady for those conditions.

DOI: 10.13009/EUCASS2019-244

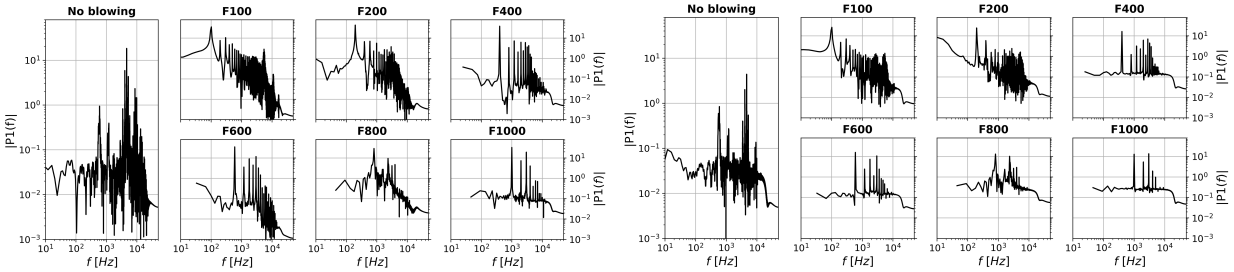

Figure 8: Frequency spectrum of the near-wake profiling point (left) and far-wake profiling point (right). Subsonic regime, $C_b = 0.95$. Constant flowing frequency sprectrum is ommited as the flow is steady for those conditions.

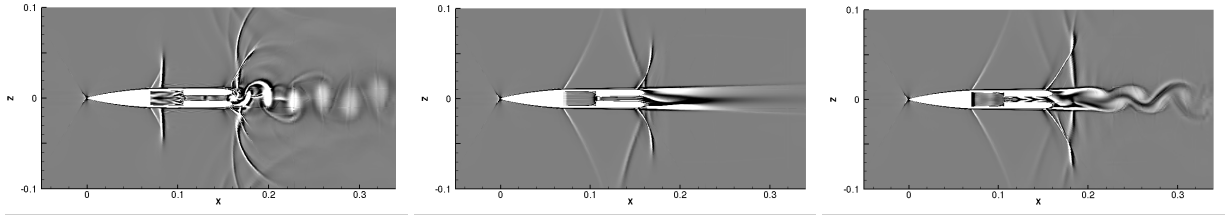

Figure 9: Shadowgraph contours of time snapshots for a transonic non-blowing configuration (left), constant blowing (center) and pulsating blowing (right).

3.2 Transonic conditions

The analysis in transonic conditions is particular to the model configuration, as the blockage effect generated by the proximity of the tunnel walls plays a major role on the flow topology around and downstream the model. Figure 9 shows a comparison between non-blowing, blowing and pulsating flow configurations, making evident the differences and changes in the compression waves distribution. If no base bleed is applied, a pair of symmetric normal shock waves appear at mid chord position of the model, as the flow adapts through the reduction of the tunnel section. The main stream accelerates up to Mach=1.1 at the trailing edge, where it separates in alternate manner from upper and lower sides, generating a complex shock wave system with normal shock waves at the trailing edge, and a pair of travelling shock waves that move up and downstream following the detachment of the eddies from the trailing edge. The application of constant blowing eliminates the vortex shedding, hence increasing the mass flow through the tunnel and making the shock waves over the model more oblique. The trailing edge shock waves have a less pronounced angle at their foot, but quickly recover a normal shape as they distance from the model. The lambda shape at the shock foot appears non-symmetric fue to the induced *Coanda* effect of the coolant jet, which forces the flow to impact the lower shear layer. When pulsating base bleed is applied, the trailing edge shock waves become more oblique, and the normal shock waves of the wake are more distanced downstream. The vortex shedding reappears with lower frequency, but with the eddies detaching downstream the wake normal shock wave, rather than from the model trailing edge.

Figure 10 depicts a series of shadowgraph snapthots to analyze the evolution of the flow topology during an injection period. When no injection is applied, the flow is almost symmetric, and the vortex shedding is diffusing downstream. As the injection begins ($t = 1/6T$), the shear layers open up generating a strong response on the trailing edge shock wave, that becomes more normal, which is coupled with the apparition of the wake normal shocks downstream the model. Full intensity injection ($t = 2/6T$ and $t = 3/6T$) show a more oblique trailing edge shock together with the detachment of a pair of eddies behind the wake normal shock waves. The damping of the injection is accompanied by a strong adaptation of the fluid in the near-wake area, again making the trailing shock waves less oblique, to finally recover the initial state with the diffusion of the eddies downstream.

Due to the unique flow topology of the non-blowing configuration (highly unstable and with strong blockage effects), the analysis of the trailing edge shock wave and drag forces statistics has been done comparing the pulsating base bleed simulations with those with constant base bleed flow values for the two coolant jet intensities. For the chosen frequencies, the constant base bleed flow offers steady references values upon which an analysis on the effect of pulsating base bleed is more clear. The results, shown in Figure 11, show a clear reduction of the shock wave angle and intensity with the application of pulsating base bleed. The relation with the frequency of injection is however not linear, indicating first an attenuation on the shock wave intensity up to frequencies of 400Hz, but recovering intensity for higher frequencies, up to values closer to the reference scenario. The magnitude of the oscillations of the shock wave

DOI: 10.13009/EUCASS2019-244

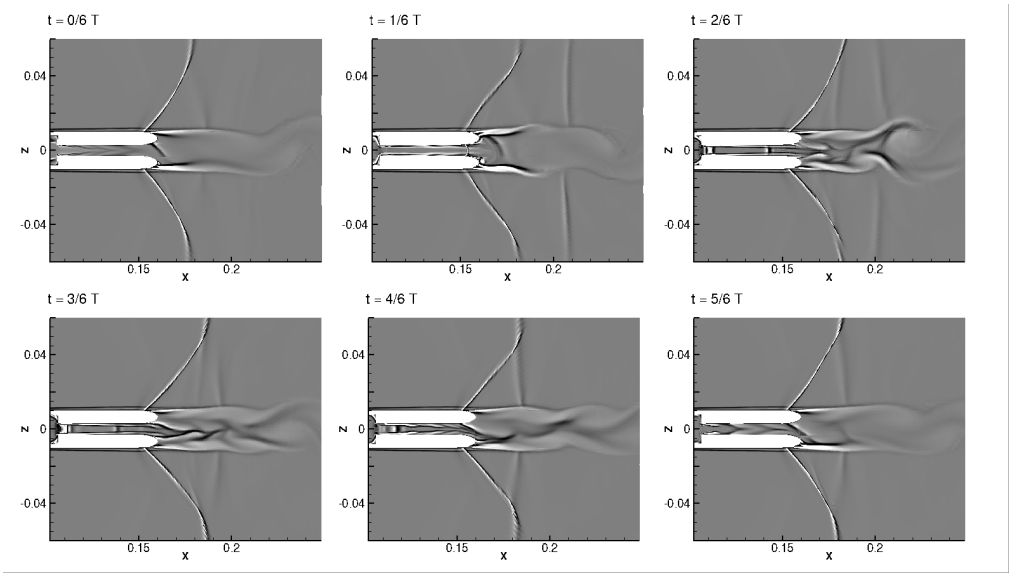

Figure 10: Shadowgraph contours time snapshots taken along a period of actuation. Transonic regime, $C_b = 0.8$, $F = 400Hz$

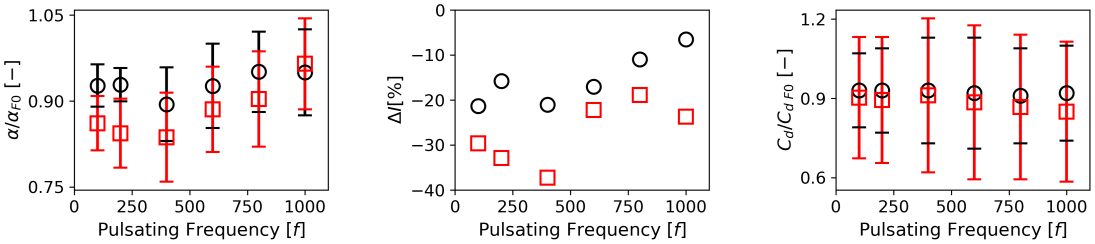

Figure 11: Influence of the pulsating base bleed in a transonic configuration. Variations of shock angle (left), shock intensity (center) and drag coefficient (right). Circular symbols (◯) are used for blowing intensities of $C_b = 0.6$, and square symbols (□) for $C_b = 0.8$. Average values with error bars (RMS) are shown for all the cases.

angle remains similar for the different frequencies, presenting again a recovering on the mean shock wave angle for frequencies above 600Hz. Mean drag values suffer minor variations, with magnitude oscillations of 20% the reference value.

The frequency spectrum analyses of the wake profiles on Figures 13 and 14 reveal a very scattered range of frequencies with high amplitude response for a non blowing configuration. A thorough analysis of the flow field, schematized in Figure 12, reveals the different phenomena present in this configuration. Oscillations due to the movement of the mid chord and trailing shock waves of upper and lower sides of the model generate low frequency perturbations, whereas high frequency oscillations are related to the interaction of upper and lower trailing edge shear layers. Small counter rotating eddies with high vorticity are generated inside the base region in the mixing area generated by the shear layers, that propagate downstream joining the main trailing edge vortices. The downstream vortex shedding, with $St = 0.26$, is clearly identified and correlated with the oscillations in the lift force exerted on the model. The frequency spectrum of actuated base bleed shows a clear dominance on the frequency of actuation and its harmonics, with scattering at high frequencies that the authors attribute to the generation of small scales vortices with high frequency due to the shear layers interaction.

3.3 Supersonic conditions

For an inflow Mach number of 2.0, the flow is dominated by a complex system of expansion and compression waves. At the trailing edge the boundary layers separate in a couple of shear layers that join again downstream forming a large recirculation area behind the body. At the same time, the main flow expands through a Prandtl-Meyer expansion fan that contacts the reflected leading edge shock wave, which looses intensity and fairly interact with the trailing edge shock wave, which has its foot at the boundary layer detachment point. This last extends to the end of the domain, interacting

DOI: 10.13009/EUCASS2019-244

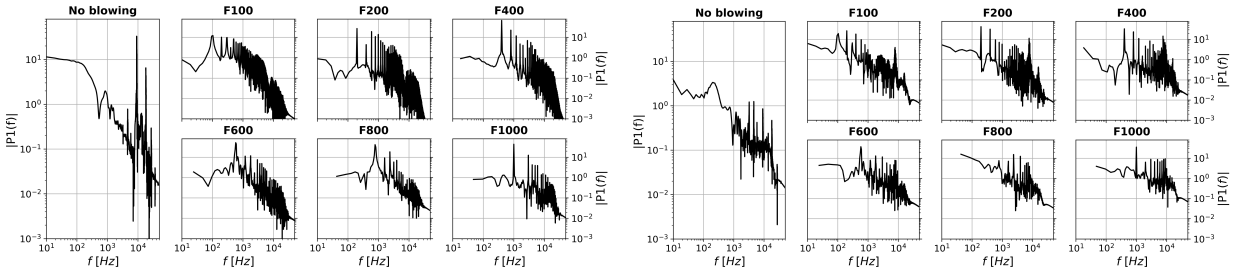

Figure 13: Frequency spectrum of the near-wake profiling point (left) and far-wake profiling point (right). Transonic regime, $C_b = 0.6$.

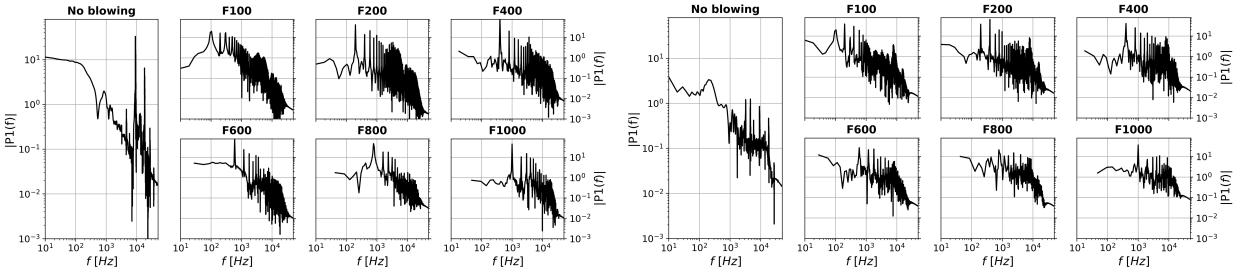

Figure 14: Frequency spectrum of the near-wake profiling point (left) and far-wake profiling point (right). Transonic regime, $C_b = 0.8$.

with another and further oblique shock wave formed at the end of the recirculation region. For both, non-blowing and constant blowing configurations, the flow solutions converge to an steady state.

Shadowgraph visualizations during a periodic base bleed actuation are shown in Figure 15. The low frequency actuation permits to observe the changes induced in the flow throughout the actuation period. From a symmetric configuration, the start of the coolant ejection ($t = 1/6T$) induces an initial wake mixing that is quickly damped. At this point ($t = 3/6T$), the *Coanda* effect is clearly visible, and the foot of the lower shock presents a marked lambda shape related with the interaction of the shear layer with the shock wave. The end of the ejection is followed by an additional mixing effect ($t = 3/6T$), that is finally damped to recover the initial state. Each of the aforementioned wake mixing effects are accompanied by large oscillations of the wake shock waves, that interact in an alternate manner with the trailing edge shock wave varying its angle along the injection period.

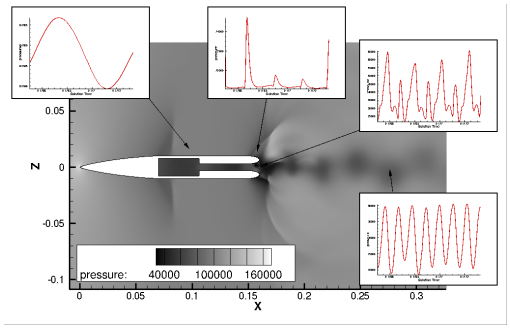

Figure 12: Identification of the diverse scales of oscillations present in the flow field, for a transonic non-blowing configuration. Contour field and plots represent static pressure values. All the plots have the same timescale.

The drag forces measured over the model did not show significant variances with the application of pulsating base bleed. For all the considered cases, variations on less than one drag count were observed during the actuation. The downstream flow, however, was deeply impacted by the coolant ejection. Figure 16 shows the relation of the shock wave angle and intensity with the frequency of actuation, together with the variations on the wake total pressure linked to these changes. As it was observed by Saracoglu et al.,[6] the application of constant trailing edge blowing has a great impact on the trailing edge shock wave, that becomes less normal and close to an 80% less strong. However, what it was not mentioned at that point, was the increment on pressure losses downstream the model, measured here as higher than 10%, compared with a non-blowing scenario. The application of pulsating base bleed reduces the damping on the shock wave intensity, leaving it about 40% weaker than the non-blowing case, but conditioned to large angle oscillations. The statistics of the shock wave angle show variations higher than 30% with respect to the mean value for some cases, generated by the oscillations generated during the wake mixing effects mentioned above. We confirm the results previously shown by Saracoglu et al.,[7] where it was shown that the frequencies of oscillations of the shock waves correspond with the pulsating base bleed frequencies. An important

DOI: 10.13009/EUCASS2019-244

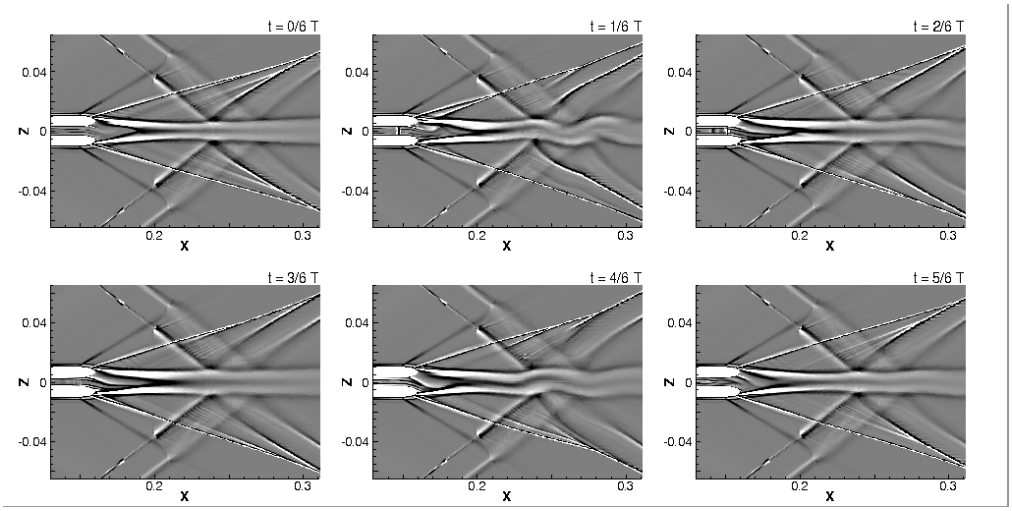

Figure 15: Shadowgraph contours time snapshots taken along a period of actuation. Supersonic regime, $C_b = 0.14$, $F = 200Hz$.

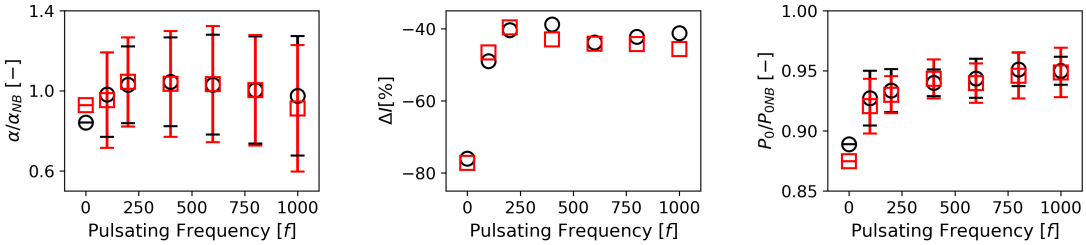

Figure 16: Influence of the pulsating base bleed in a supersonic configuration. Variations of shock angle (left), shock intensity (center) and wake total pressure losses (right). Circular symbols (◯) are used for blowing intensities of $C_b = 0.14$, and square symbols (□) for $C_b = 0.2$. Average values with error bars (RMS) are shown for all the cases.

point to remark, is that these variations are measured at a distance equivalent of the model length downstream the trailing edge.

The analysis of the frequency spectrum of the wake oscillations reveal a clear dependency of the variations with the pulsating frequency in the near-wake region. Figures 17 and 18 indicate how the base bleed frequency and its harmonics dominate above higher frequency oscillations. In the far-wake region, high frequency variations are detected for all the configurations, which can be related to the development of the turbulent wake as the eddies travel downstream, where the smaller scales have higher associated frequencies.

DOI: 10.13009/EUCASS2019-244

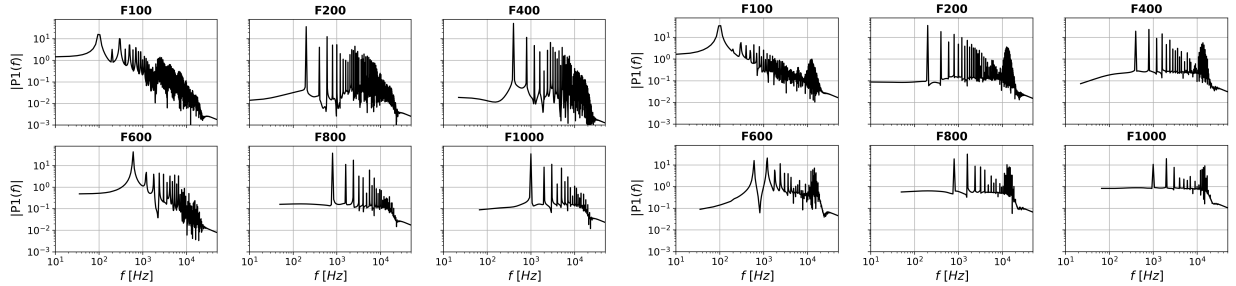

Figure 17: Frequency spectrum of the near-wake profiling point (left) and far-wake profiling point (right). Supersonic regime, $C_b = 0.14$. Constant flowing frequency sprectrum is ommited as the flow is steady for those conditions.

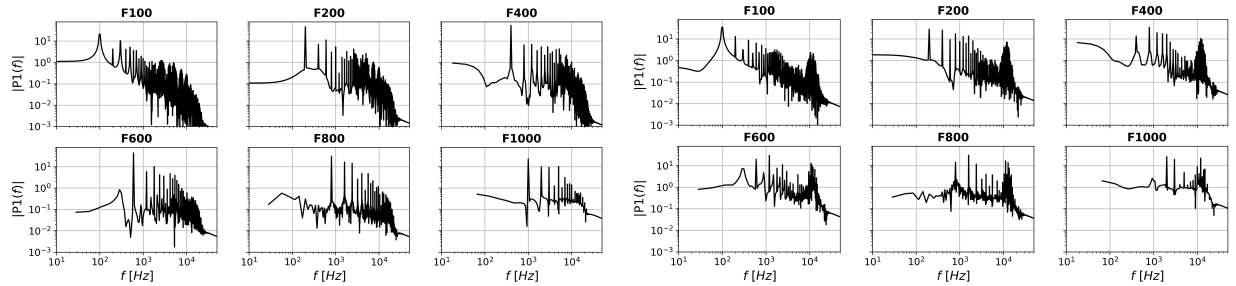

Figure 18: Frequency spectrum of the near-wake profiling point (left) and far-wake profiling point (right). Supersonic regime, $C_b = 0.2$. Constant flowing frequency sprectrum is ommited as the flow is steady for those conditions.

4. Conclusions

The complexity of trailing edge flow, with different scales and interactions occurring simultaneously, can compromise the aerodynamic performance of transonic and supersonic outlet turbines. A thorough investigation of the effects of pulsating base bleed has been conducted and compared with constant blowing and non-blowing configurations, covering from the subsonic to the supersonic regime. The numerical analysis contemplated a model inside the tunnel, aiming to replicate these analyses in experimental campaigns, and hence serving these results as the base for the design of experiments. Furthermore, a valuable database of unsteady flow has been generated to properly address future experimental campaigns. The potential capabilities of trailing edge flow control are notable, as the ejection of cooling flow has proven to be very effective in the modulation of downstream flow structures. Base pressure gains have been observed to be always higher for constant blowing, but the modulation of wake and shock structures achieved with pulsed blowing is measurable one chord downstream the model. Moreover, the oscillations of the flow structures appear to be in phase with the intermittent injection frequency, enabling possible flow feature control on the interaction with downstream elements of the turbine. The description and capabilities shown here will hopefully contribute to support turbine blade designers on the optimization of secondary flows and blade cooling as well as its interaction with different stages of the system.

5. Acknowledgements

This research has being carried out under the project SSeMID (*Stability and Sensitivity Methods for Industrial Design*, http://ssemid-itn.eu/), which has received funding from the European Union Horizon 2020 research and innovation programme under the Marie Skłodowska-Curie grant agreement No 675008.

The author acknowledges the computer resources and technical assistance provided by the Centro de Supercomputación y Visualización de Madrid (CeSViMa)

DOI: 10.13009/EUCASS2019-244

References

[1] J. D. Denton and L. Xu, "The Trailing Edge Loss of Transonic Turbine Blades," *Journal of Turbomachinery*, vol. 112, no. 2, pp. 277–285, 1990.

[2] F. Motallebi and J. Norbury, "The effect of base bleed on vortex shedding and base pressure in compressible flow," *Journal of Fluid Mechanics*, vol. 110, pp. 273–292, 1981.

[3] F. H. Kost and A. T. Holmes, "Aerodynamic effect of coolant ejection in the rear part of transonic rotor blades," in *AGARD Heat transfer and Cooling in Gas Turbines 12 p (SEE N86-29823 21-07)*, 1985.

[4] M. Raffel and F. Kost, "Investigation of aerodynamic effects of coolant ejection at the trailing edge of a turbine blade model by PIV and pressure measurements," *Experiments in Fluids*, vol. 24, no. 5-6, pp. 447–461, 1998.

[5] Z. Yang and H. Hu, "An experimental investigation on the trailing edge cooling of turbine blades," *Propulsion and Power Research*, vol. 1, no. 1, pp. 36–47, 2012.

[6] B. H. Saracoglu, G. Paniagua, J. Sanchez, and P. Rambaud, "Effects of blunt trailing edge flow discharge in supersonic regime," *Computers & Fluids*, vol. 88, pp. 200–209, dec 2013.

[7] B. H. Saracoglu, G. Paniagua, S. Salvadori, F. Tomasoni, S. Duni, T. Yasa, and A. Miranda, "Trailing edge shock modulation by pulsating coolant ejection," *Applied Thermal Engineering*, vol. 48, no. April, pp. 1–10, 2012.

[8] C. Bernardini, S. Salvadori, F. Martelli, G. Paniagua, and B. H. Saracoglu, "Pulsating Coolant Ejection Effects Downstream of Supersonic Trailing Edge," *Engineering Applications of Computational Fluid Mechanics*, vol. 7, pp. 250–260, jan 2013.

[9] J. Saavedra, G. Paniagua, and B. H. Saracoglu, "Experimental Characterization of the Vane Heat Flux Under Pulsating Trailing-Edge Blowing," *Journal of Turbomachinery*, vol. 139, no. 6, p. 061004, 2017.

[10] G. Paniagua, B. Saracoglu, F. Tomasoni, S. Salvadori, A. Miranda, and F. Martelli, "Modulation of Vane Shocks with Pulsating Coolant Flows," in *47th AIAA/ASME/SAE/ASEE Joint Propulsion Conference & Exhibit*, (Reston, Virigina), American Institute of Aeronautics and Astronautics, jul 2011.

[11] A. Martinez-Cava, E. Valero, J. de Vicente, and G. Paniagua, "Coanda Flow Characterization on Base Bleed Configurations Using Global Stability Analysis," in *AIAA Scitech 2019 Forum*, (San Diego, California), pp. 1–17, American Institute of Aeronautics and Astronautics, jan 2019.

[12] A. Martinez-Cava, Y. Wang, J. de Vicente, and E. Valero, "Pressure Bifurcation Phenomenon on Supersonic Blowing Trailing Edges," *AIAA Journal*, vol. 57, pp. 153–164, jan 2019.

[13] G. Paniagua, D. Cuadrado, J. Saavedra, V. Andreoli, D. Lawrence, T. Meyer, and S. Meyer, "Design of the Purdue Experimental Turbine Aerothermal Laboratory for Optical and Surface Aero-Thermal Measurements," *Proceedings of ASME Turbo Expo 2016*, pp. 1–13, 2016.

[14] D. Schwamborn, T. Gerhold, and R. Heinrich, "The DLR Tau-code: Recent Applications in Research and Industry," in *ECCOMAS CFD 2006: Proceedings of the European Conference on Computational Fluid Dynamics*, Edmond aan Zee, Netherlands: Delft University of Technology, 2006.

[15] D. C. Wilcox, "Formulation of the k-w Turbulence Model Revisited," *AIAA Journal*, vol. 46, pp. 2823–2838, nov 2008.